ISSN NO. 2320-5407

Journal homepage: http://www.journalijar.com

INTERNATIONAL JOURNAL OF ADVANCED RESEARCH

RESEARCH ARTICLE

Corrosion Protection of Carbon Steel in Hydrochloric Acid Solutions using Heterocyclic Compounds

***A. S. Fouda[*1], A. M. El-Desoky[2] M. A. Diab[3], A. H.Soliman[1]**

1. Department of Chemistry, Faculty of Science, El-Mansoura University, El-Mansoura-35516, Egypt
2. Engineering Chemistry Department, High Institute of Engineering & Technology (New Damietta) , Egypt,
3. Department of Chemistry, Faculty of Science, Damietta University, Dameitta, Egypt

Manuscript Info

Manuscript History:

Received: 12 January 2014
Final Accepted: 23 February 2014
Published Online: March 2014

Key words:
:Corrosion inhibition; carbon steel; HCl, EFM, EIS, SEM–EDX

Corresponding Author

A. S. Fouda

Abstract

The role of some heterocyclic compounds (1-3) as corrosion inhibitors for C-steel in 1 M HCl have been studied using weight loss, potentiodynamic polarization, electrochemical impedance spectroscopy (EIS) and electrochemical frequency modulation (EFM) techniques. Polarization studies showed that all the compounds studied are mixed type inhibitors. The effect of temperature on corrosion inhibition has been studied and the thermodynamic activation and adsorption parameters were calculated and discussed. Electrochemical impedance was used to investigate the mechanism of corrosion inhibition. The presence of these compounds in the solution decreases the double layer capacitance and increases the charge transfer resistance. The adsorption of these compounds on C-steel surface was found to obey Temkin's adsorption isotherm. The morphology of inhibited and uninhibited C- steel was analyzed by scanning electron microscope (SEM) and energy dispersive X-ray spectroscopy (EDX)

1. Introduction

Acid solutions are widely used in industry, the most important fields of application being acid pickling, industrial acid cleaning, acid decaling and oil well acidizing. Because of the general aggressivity of acid solutions, inhibitors are commonly used to reduce the corrosive attack on metallic materials. Most of the well-known acid inhibitors are organic compounds containing N, O, P, S and aromatic ring or triple bonds. It was reported before that the inhibition efficiency decreases in the order: O < N < S [1-4]. In general, organic compounds are effective inhibitors of aqueous corrosion of many metals and alloys. The use of chemical inhibitors to decrease the rate of corrosion processes of carbon steels is quite varied [5-9]. A variety of organic compounds containing heteroatoms such as O, N, S and multiple bonds in their molecule are of particular interest as they give better inhibition efficiency than those containing N or S alone [10-11]. Sulfur and/or nitrogen containing heterocyclic compounds with various substituents are considered to be effective corrosion inhibitors. Hydrazide derivatives offer special affinity to inhibit corrosion of metals in acid solutions [12-15]. Indole derivatives [32–34], benzimidazole derivatives [35–39] were used as corrosion inhibitors for metals and alloys, the purpose of this paper is to compare the corrosion inhibition data derived from EFM with that obtained from Tafel extrapolation, EIS and weight loss techniques. Also, the morphology of carbon steel surfaces was investigated by SEM and EDX.

2- Experimental detail

2.1- Composition of material samples

2.2- Chemicals and solutions

2.2.1- Chemicals

Hydrochloric acid (BDH grade) and organic additives (inhibitors) used in this study were some heterocyclic compounds, listed in the following Table (2)

2.3- Methods used for corrosion measurements

2.3.1. Weight loss measurements

For weight loss measurements, square specimens of size 2 x 2 x 0.2 cm were used. The specimens were abraded with emery papers grit sizes (400,800 and 1200), degreased with acetone. Then rinsed several times with bidistilled water, and finally dried between two filter papers. The weight loss measurements were carried out in a 100 ml capacity glass beaker placed in a water thermostat bath. The specimens were then immediately immersed in the test solution without or with desired concentration of the investigated compounds. Triplicate specimens were exposed for each condition and the mean weight losses were reported. The degree of surface coverage (θ) and inhibition efficiency (% IE) were calculated from equation (1):

$$\% IE = \theta \times 100 = [\text{Weight loss}_{(pure)} - \text{Weight loss}_{(inh.)} / \text{Weight loss}_{(pure)}] \times 100 \quad (1)$$

2.3.2. Potentiodynamic polarization measurements

Polarization experiments were carried out in a conventional three-electrode cell with a platinum counter electrode (1 cm^2) and a saturated calomel electrode (SCE) coupled to a fine Luggin capillary as the reference electrode. The working electrode was in the form of a square cut from C-steel sheet embedded in epoxy resin of polytetrafluoroethylene so that the flat surface area was 1 x 1 cm. The working electrode was abraded with emery papers grit sizes up to 1200. Before measurement, the electrode was immersed in solution at open potential for 30 min. until a steady state was reached. The potential was started from - 500 to + 500 mV vs. open circuit potential (E_{op}). All experiments were carried out in freshly prepared solutions at room temperature and results were always repeated at least three times to check the reproducibility. The degree of surface coverage (θ) and inhibition efficiency (% IE) were calculated from equation (2):

$$\% IE = \theta \times 100 = [1 - i_{corr(inh)}/i_{corr(free)}] \times 100 \quad (2)$$

where $i_{corr(free)}$ and $i_{corr(inh)}$ are the current densities in the absence and presence of inhibitor, respectively.

2.3.3. Electrochemical impedance spectroscopy measurements

All EIS measurements were performed at open circuit potential E_{ocp} at 25 ±1°C over a wide frequency range of (20 kHz to 0.08 Hz). The sinusoidal potential perturbation was 10 mV in amplitude peak to peak. The degree of surface coverage (θ) and inhibition efficiency (% IE) were calculated from equation (3):

$$\% IE = \theta \times 100 = [1 - R_{ct(free)} /R_{ct(inh)}] \times 100 \quad (3)$$

where $R_{ct(free)}$ and $R_{ct(inh)}$ are the charge transfer resistances in the absence and presence of inhibitor, respectively.

2.3.4. Electrochemical frequency modulation measurements

EFM experiments were performed with applying potential perturbation signal with amplitude 10 mV with two sine waves of 2 and 5 Hz. The choice for the frequencies of 2 and 5Hz was based on three arguments [22]. The larger peaks were used to calculate the corrosion current density (i_{corr}), the Tafel slopes (β_c and β_a) and the causality factors CF-2 and CF-3 [23].

All electrochemical experiments were carried out using Gamry instrument PCI300/4 Potentiostat/Galvanostat/Zra analyzer, DC105 Corrosion software, EIS300 EIS software, EFM140 EFM software and Echem Analyst 5.5 for results plotting, graphing, data fitting and calculating. The degree of surface coverage (θ) and inhibition efficiency (% IE) were calculated as in the potentiodynamic polarization [equation (2)]:

2.3.5. SEM-EDX measurements

The C-steel surface was prepared by keeping the specimens for 12 hrs in 1 M HCl in presence and absence of optimum concentration of heterocyclic compounds, after abraded mechanically using different grades of emery papers up to 1200 grit size. Then, after this immersion time, the specimens were washed gently with bidistilled water, carefully dried and mounted into the spectrometer without any further treatment.

The corroded C-steel surfaces were examined using an X-ray diffractometer Philips (pw-1390) with Cu-tube (Cu Ka1, l = 1.54051 A °), a scanning electron microscope (SEM, JOEL, JSM-T20, Japan).

2.3.6. Theoretical study
Accelrys (Material Studio Version 4.4) software for quantum chemical calculations has been used.

3. Results and Discussion

3.1. Weight loss measurements

Weight loss of C-steel, in mg cm^{-2} of the surface area, was determined at various time intervals in the absence and presence of different concentrations (11×10^{-6}- 21×10^{-6} M) of the additives (1-3). The curves obtained in the presence of different concentrations of inhibitor (1) fall significantly below that of free acid (Fig.1). Similar behaviors were obtained for the other additives. Values of % IE are tabulated in Table (1). In all cases, the increase in the inhibitor concentration was accompanied by a decrease in the weight loss and an increase in % IE. These results lead to the conclusion that, these compounds under investigation are fairly efficient inhibitors for C-steel dissolution in HCl solution. Careful inspection of these results showed that, at the same inhibitor concentration, the % IE of the inhibitors increases as follows: 1 < 2 < 3

Table (1): Chemical composition (weight %) of the carbon steel

Element	C	Mn	P	Si	Fe
Weight (%)	0.200	0.350	0.024	0.003	rest

Table (2): Chemical structures, names, molecular formulas and molecular weights of inhibitors

Comp.	Structures	Names	Mol. Formulas Mol. Weights
1	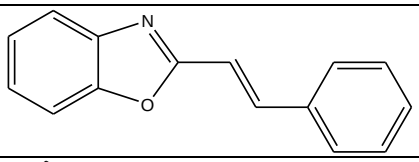	2-styrylbenzo[d] oxazole	$C_{15}H_{11}NO$ 221.2539
2	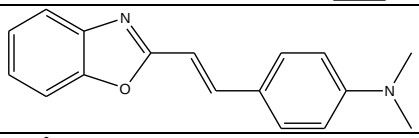	4-((E)-2-(benzo[d] oxazol-2-yl)vinyl)-N,N-dimethyl benzenamine	$C_{17}H_{16}N_2O$ 264.3217
3	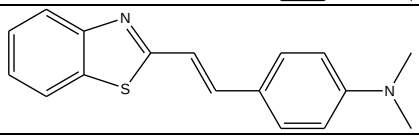	4-((E)-2-(benzo[d]thiazol-2-yl)vinyl)-N,N-dimethyl benzenamine	$C_{17}H_{16}N_2S$ 280.3873

Table (1): Variation of inhibition efficiency (% IE) of different compounds with their molar concentrations from weight loss measurements at 120 min immersion in 1 M HCl at 30 °C

Conc. (M)	inhibition efficiency (% IE)		
	1	2	3
11 x 10^{-6}	29.41	42.11	52.63
13 x 10^{-6}	35.29	47.37	58.34
15 x 10^{-6}	43.61	52.17	68.42
17 x 10^{-6}	47.54	56.55	73.68
19 x 10^{-6}	52.94	60.48	76.75
21 x 10^{-6}	58.82	68.42	81.96

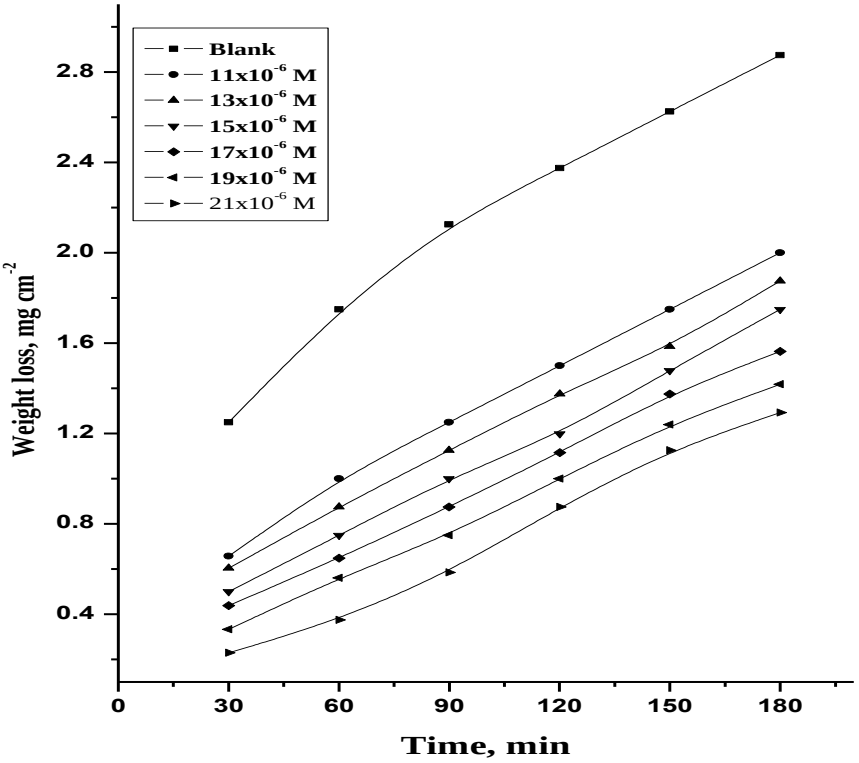

Figure (1): Weight –loss time curves for the dissolution of C-steel in the absence and presence of different concentration of compound (1) at 30°C

3.1.1. Adso

Assuming the corrosion inhibition was caused by the adsorption of organic derivatives, and the values of surface coverage for different concentrations of inhibitors in 1 M HCl were evaluated from weight loss measurement using equation (1)

From the values of (θ), it can be seen that the values of (θ) increased with increasing the concentration of heterocyclic compounds. Using these values of surface coverage, one can utilize different adsorption isotherms to deal with experimental data. The Temkin adsorption isotherm was applied to investigate the adsorption mechanism, by plotting (θ) vs. log C, straight lines were obtained (Figure 2). The isotherm is described by the following equation:

$$\theta = 2.303/a \log K_{ads} + 2.303/a \log C \quad (4)$$

where C is inhibitor concentration, K_{ads} is equilibrium constant of adsorption and 'a' is the heterogeneity factor. It is well known that the standard adsorption free energy ($\Delta G°_{ads}$) is related to equilibrium constant of adsorption (K_{ads}) by the following equation [24]:

$$K_{ads} = 1/55.5 \exp [-\Delta G°_{ads}/RT] \quad (5)$$

The thermodynamic parameters for the adsorption process that were obtained from this Figure are shown in Table (2). The values of □ $G°_{ads}$ are negative and increased as the % IE increased which indicates that these investigated compounds are strongly adsorbed on the C- steel surface and show the spontaneity of the adsorption process and stability of the adsorbed layer on the C-steel surface. Generally, values of □ $G°_{ads}$ up to □ 20 kJ mol^{-1} are consistent with the electrostatic interaction between the charged molecules and the charged metal (physical adsorption) while those more negative than □ 40 kJ mol^{-1} involve sharing or transfer of electrons from the inhibitor molecules to the metal surface to form a coordinate type of bond (chemisorptions) [25]. The values of □ $G°_{ads}$ obtained were approximately equal to □ □ □ □ kJ mol^{-1} indicating that the adsorption mechanism of the investigated compounds on C- steel in 1 M HCl solution involves both electrostatic adsorption and chemisorptions [26]. The thermodynamic

parameters point toward both physisorption (major contributor) and chemisorptions (minor contributor) of the inhibitors onto the metal surface. The K_{ads} follows the same trend in the sense that large values of K_{ads} imply better more efficient adsorption and hence better inhibition efficiency [27].

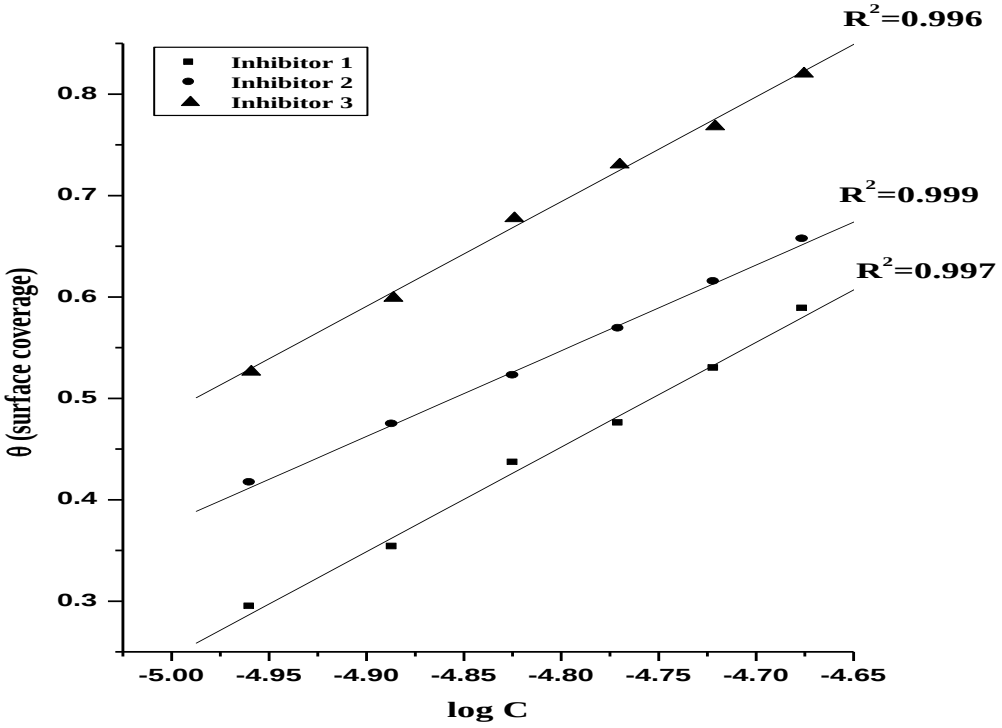

Figure (2): Kinetic model isotherm curves for the dissolution of C-steel in the presence of different concentration of investigated compounds

Table (2): Parameters obtained from Temkin adsorption isotherm and kinetic model for C- steel in 1 M HCl for investigated compounds

Compound	Temkin			Kinetic model		
	a	K_{ads}, M^{-1}	$-\Delta G°_{ads}$, kJ mol^{-1}	1/y	K_{ads}, M^{-1}	$-\Delta G°_{ads}$, kJ mol^{-1}
1	2.218	172048.5	40.49	0.53	56642.04	32.32
2	2.724	279881.8	41.72	0.62	71750.11	40.94
3	2.23	296416.7	41.87	0.46	93360.96	53.27

3.1.2. Effect of temperature

Corrosion reactions are usually regarded as Arrhenius processes and the rate (k) can be expressed by the relation:

$$k = A \exp (E_a/RT) \quad (6)$$

where E_a is the activation energy of the corrosion process R is the universal gas constant, T is the absolute temperature and A is a Arrhenius pre-exponential constant depends on the metal type and electrolyte. Arrhenius plots of log k vs. 1/T for carbon steel in 1 M HCl in the absence and presence of 21 x 10^{-6} M of different inhibitors are shown graphically in Figure 3. The variation of log k vs. 1/T is a linear one and the values of E_a obtained are summarized in Table (3). These results suggested that the inhibitors are similar in the mechanism of action. The increase in E_a with the addition of concentration of inhibitors (1-3) indicating that the energy barrier for the corrosion reaction increases. It is also indicated that the whole process is controlled by surface reaction, since the activation energy of the corrosion process is over 14 kJ mol^{-1} [28].

Enthalpy and entropy of activation (ΔH°, ΔS°) are calculated from transition state theory using the following equation [29]:

$$k = \frac{RT}{Nh} \exp\left(\frac{\Delta S^{\circ}}{R}\right) \exp\left(\frac{\Delta H^{\circ}}{RT}\right) \quad (7)$$

where h is Planck's constant, N is Avogadro's number. A plot of log k/T vs 1/T also gave straight lines as shown in Fig. 4 for carbon steel dissolution in 1 M HCl in the absence and presence of 21 x 10^{-6} M of different inhibitors. The slopes of these lines equal $-\Delta H^{\circ}/2.303R$ and the intercept equal log RT/Nh + (ΔS°/2.303R) from which the value of ΔH° and ΔS° were calculated and tabulated in Table (3). From these results, it is clear that the presence of the investigated compounds increased the activation energy values and consequently decreased the corrosion rate of the carbon steel. These results indicate that these investigated compounds acted as inhibitors through increasing activation energy of carbon steel dissolution by making a barrier to mass and charge transfer by their adsorption on carbon steel surface. The values of ΔH° reflects the strong adsorption of these compounds on carbon steel surface. The values of ΔS° in absence and presence of the tested compounds are large and negative; this indicates that the activated complex in the rate-determining step represents an association rather than dissociation step, meaning that a decreases in disordering takes place on going from reactants to the activated complex and the activated molecules were in higher order state than that at the initial state [30, 31].

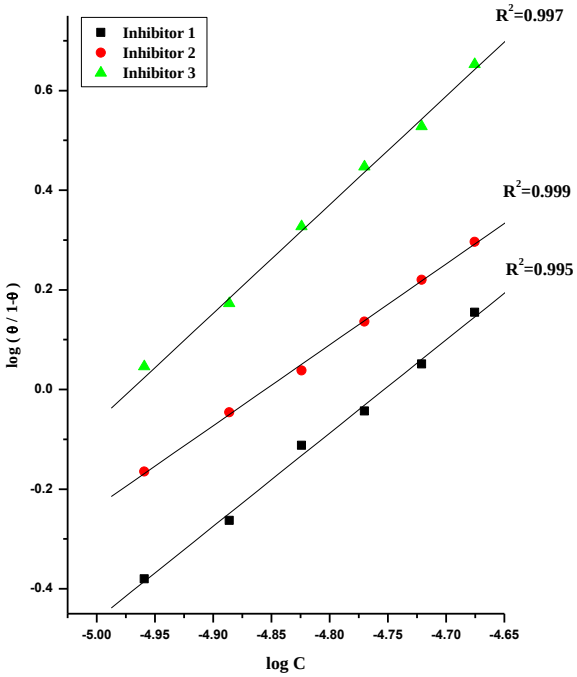

Figure (3): Kinetic model isotherm curves for the dissolution of C-steel in the presence of different concentration of investigated compounds

Table (3): Activation parameters of the dissolution of C-steel in 1 M HCl in the absence and presence of $21x10^{-6}$ M of investigated inhibitors

Inhibitor	Activation Parameters		
Blank	E_a^*, kJ mol^{-1}	ΔH^*, kJ mol^{-1}	$-\Delta S^*$, J mol^{-1} K^{-1}
	14.53	5.19	141.2
Compound 1	15.72	5.70	255.30
Compound 2	26.17	10.24	255.19
Compound 3	43.10	40.6	254.86

3.2. Potentiodynamic polarization measurements

Anodic and cathodic polarizations were carried out potentiodynamic in unstirred 1 M HCl solution in the absence and presence of various concentrations of the inhibitors (1- 3) at 303 K over potential range 300 mV ± OCP. The results are represented in Fig. 5 for compound (1). Similar behaviors were obtained for other compounds. The obtained potentiodynamic polarization parameters are given in Table (4). These results indicate that the cathodic and anodic curves obtained exhibit Tafel-type behavior. Additionally, the form of these curves is very similar either in the cathodic or in the anodic side, which indicates that the mechanisms of carbon steel dissolution and hydrogen reduction apparently remain unaltered in the presence of these additives. Addition of investigated compounds decreased both the cathodic and anodic current densities and caused mainly parallel displacement to the more negative and positive values, respectively, i.e. the presence of investigated compounds in solution inhibits both the hydrogen evolution and the anodic dissolution processes with overall shift of E_{corr} to more negative values with respect to the OCP.

The results also show that the slopes of the anodic and the cathodic Tafel lines (β_a and β_c) were slightly changed on increasing the concentration of the tested compounds. This indicates that there is no change of the mechanism of inhibition in presence and absence of inhibitors and indicates that these compounds acted as mixed type inhibitors, but the cathode is more preferentially polarized than the anode. The higher values of Tafel slope can be attributed to surface kinetic process rather the diffusion-controlled process [32]. The constancy and the parallel of cathodic slope obtained from the electrochemical measurements indicate that the hydrogen evolution reaction was activation controlled [33] and the addition of these derivatives did not modify the mechanism of this process. This result suggests that the inhibition mode of the anhydride derivatives used was by simple blockage of the surface by adsorption.

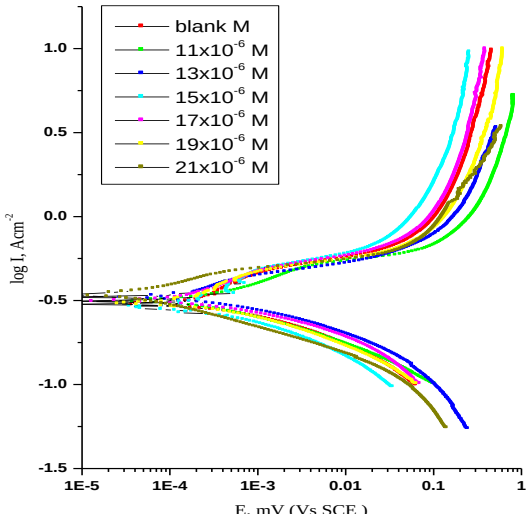

Figure (5): Potentiodynamic polarization curves for the corrosion of C- steel in 1M HCl in the absence and presence of various concentrations of compound (1) at 30°C

Table (4): The effect of concentration of the investigated compounds on the free corrosion potential (E_{corr}), corrosion current density (i_{corr}), Tafel slopes (β_a& β_c), inhibition efficiency (% IE) , and degree of surface coverage for the corrosion of C-steel in 1 M HCl at 30 °C

Comp.	Conc., M	- $E_{corr.}$, mVvs SCE	i_{corr} mA cm^{-2}	β_a , mV dec^{-1}	β_c, mV dec^{-1}	θ	% IE
1	Blank	521	120	66	77		
	11×10^{-6}	503	91	39	107	0.242	24.2
	13×10^{-6}	479	35	37	199	0.708	70.8
	15×10^{-6}	540	18	28	23	0.850	85.0
	17×10^{-6}	503	16	22	85	0.867	86.7
	19×10^{-6}	521	15	26	84	0.875	87.5
	21×10^{-6}	465	11.9	26	53	0.901	90.1
2	11×10^{-6}	412	11.3	69	77	0.906	90.6
	13×10^{-6}	433	11.1	36	66	0.908	90.8
	15×10^{-6}	431	11.0	02	127	0.908	90.8
	17×10^{-6}	470	9.5	52	61	0.921	92.1
	19×10^{-6}	436	8.8	99	114	0.926	92.6
	21×10^{-6}	500	8.5	86	95	0.929	92.9
3	11×10^{-6}	433	8.3	82	138	0.931	93.1
	13×10^{-6}	503	7.6	93	96	0.937	93.7
	15×10^{-6}	491	6.3	158	80	0.947	94.7
	17×10^{-6}	460	6.2	96	71	0.948	94.8
	19×10^{-6}	411	2.9	41	72	0.976	97.6
	21×10^{-6}	460	1.6	60	49	0.986	98.6

3.3. Electrochemical impedance spectroscopy (EIS) measurements

Impedance diagram (Nyquist) at frequencies ranging from 1 Hz to 1 kHz with 10 mV amplitude signal at OCP for carbon steel in 1 M HCl in the absence and presence of different concentrations of compounds (1-3) are obtained. The equivalent circuit that describes our metal/electrolyte interface is shown in Fig. 6 where R_s, R_{ct} and CPE refer to solution resistance, charge transfer resistance and constant phase element, respectively. EIS parameters and % IE were calculated and tabulated in Table (5). In order to correlate impedance and polarization methods, i_{corr} values were obtained from polarization curves and Nyquist plots in the absence and presence of different concentrations of compounds (1-3) using the Stern-Geary equation:

$$i_{corr} = \frac{\square_a \square_c}{2.303 (\square_a + \square_c) R_{ct}} \quad (4)$$

The obtained Nyquist plot for compound (1) is shown in Fig. 7. Each spectrum is characterized by a single full semicircle. The fact that impedance diagrams have an approximately semicircular

appearance shows that the corrosion of carbon steel is controlled by a charge transfer process. Small distortion was observed in some diagrams, this distortion has been attributed to frequency dispersion [34]. The diameters of the capacitive loop obtained increases in the presence of anhydride derivatives, and were indicative of the degree of inhibition of the corrosion process [35].

It was observed from the obtained EIS data that R_{ct} increases and C_{dl} decreases with the increasing of inhibitor concentrations. The increase in R_{ct} values, and consequently of inhibition efficiency, may be due to the gradual replacement of water molecules by the adsorption of the inhibitor molecules on the metal surface to form an adherent film on the metal surface. And this suggests that the coverage of the metal surface by the film decreases the double layer thickness. Also, this decrease of C_{dl} at the metal/solution interface with increasing the inhibitor concentration can result from a decrease in local dielectric constant which indicates that the inhibitors were adsorbed on the surface at both anodic and cathodic sites [36].

The impedance data confirm the inhibition behavior of the inhibitors obtained with other techniques. From the data of Table (5), it can be seen that the i_{corr} values decrease significantly in the presence of these additives and the % IE is greatly improved. The order of reduction in i_{corr} exactly correlates with that obtained from potentiostatic polarization studies. Moreover, the decrease in the values of i_{corr} follows the same order as that obtained for the values of C_{dl}. It can be concluded that the inhibition efficiency found from weight loss, polarization curves, electrochemical impedance spectroscopy measurements and the Stern-Geary equation are in good agreement.

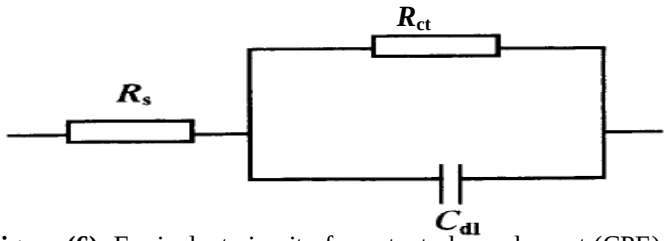

Figure (6): Equivalent circuit of constant phase element (CPE).

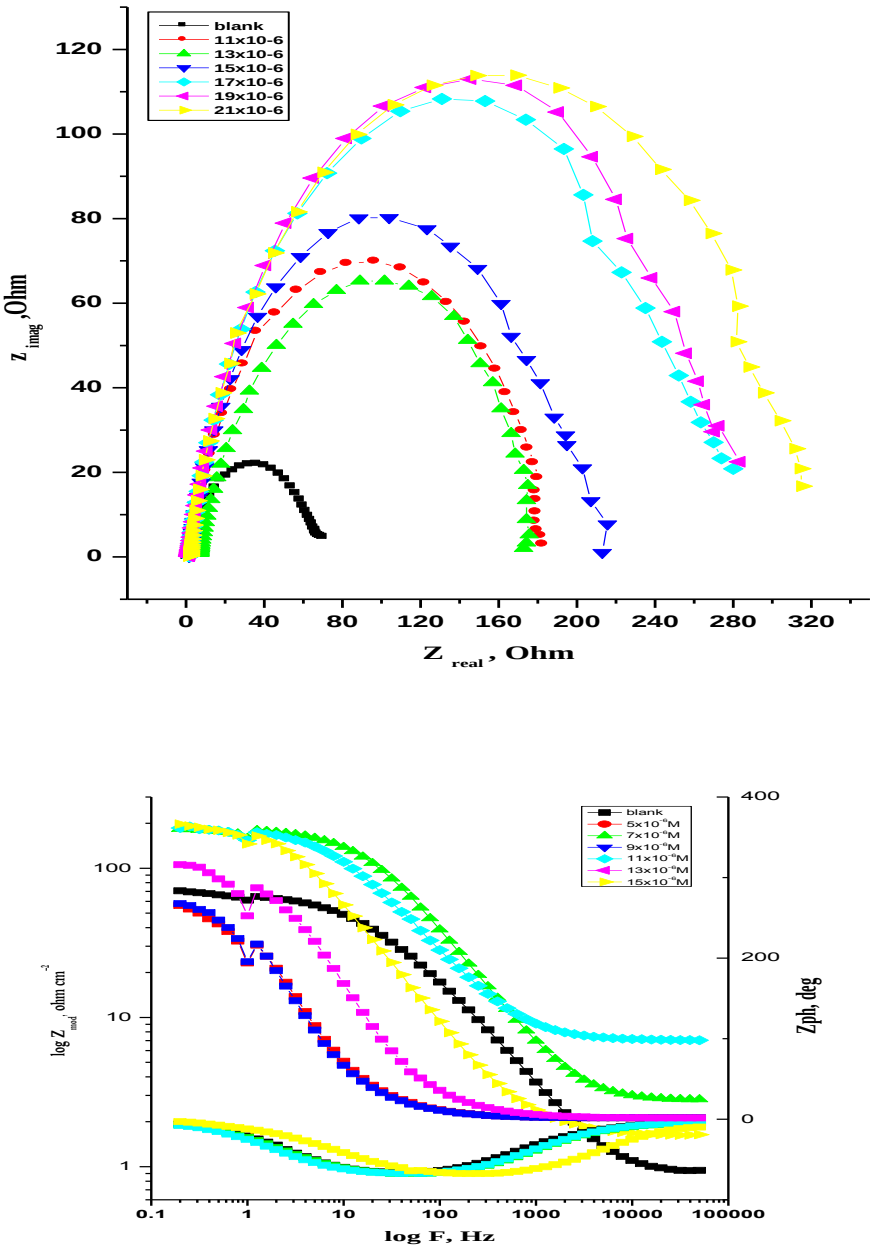

Figure (7): The Nyquist (a) and Bode (b) plots for corrosion of C-steel in 1 M HCl in the absence and presence of different concentrations of compound (1) at 30 °C

Table (5): Electrochemical kinetic parameters obtained by EIS technique for in 1 M HCl without and with various concentrations of compounds at 30°C

Comp.	Conc., M	R_s Ω cm^2	Y_o, x 10^{-3} $\mu\Omega^{-1}$ sn	n	R_{ct}, Ω cm^2	C_{dl} x 10^{-4} μFcm^{-2}	θ	% IE
1	Blank	8.572	362.3	0.7737	65.6	1.214	---	---
	11 × 10^{-6}	2.658	111.3	0.8384	178.9	0.523	0.633	63.3

	13×10^{-6}	6.756	244.3	0.7832	179.4	1.028	0.634	63.4
	15×10^{-6}	1.641	495.6	0.8399	198.1	3.184	0.669	66.9
	17×10^{-6}	1.558	392.5	0.8409	270.3	2.570	0.757	75.7
	19×10^{-6}	1.572	426.6	0.8389	278.6	2.830	0.765	76.5
	21×10^{-6}	1.418	133.3	0.8289	304.5	0.688	0.785	78.5
2	11×10^{-6}	1.229	140.1	0.8329	307.5	0.745	0.787	78.7
	13×10^{-6}	1.255	129.8	0.8289	326.4	0.676	0.799	79.9
	15×10^{-6}	1.06	136.2	0.8292	353.6	0.729	0.814	81.4
	17×10^{-6}	1.2	131.1	0.8275	354.4	0.691	0.815	81.5
	19×10^{-6}	5.079	215.1	0.8071	360.7	1.170	0.818	81.8
	21×10^{-6}	1.754	371.3	0.8196	365	2.390	0.820	82.0
3	11×10^{-6}	4.89	210.3	0.8321	424.3	1.290	0.845	84.5
	13×10^{-6}	2.189	220.1	0.8251	476.8	1.370	0.862	86.2
	15×10^{-6}	3.095	235.9	0.8177	478.4	1.450	0.863	86.3
	17×10^{-6}	2.684	242	0.8082	483	1.450	0.864	86.4
	19×10^{-6}	2.257	240.9	0.8051	489.1	1.435	0.866	86.588
	21×10^{-6}	2.158	172.2	0.8157	554.8	1.013	0.882	88.176

3.4. Electrochemical frequency modulation (EFM*)* measurements

EFM is a nondestructive corrosion measurement technique that can directly and quickly determine the corrosion current value without prior knowledge of Tafel slopes, and with only a small polarizing signal. These advantages of EFM technique make it an ideal candidate for online corrosion monitoring [37].

The great strength of the EFM is the causality factors which serve as an internal check on the validity of EFM measurement. The causality factors CF-2 and CF-3 are calculated from the frequency spectrum of the current responses. Figure (8) shows the frequency spectrum of the current response of pure carbon steel in 1 M HCl, contains not only the input frequencies, but also contains frequency components which are the sum, difference, and multiples of the two input frequencies. The EFM intermodulation spectrums of carbon steel in 1 M HCl acid solution containing ($11x10^{-6}$ M and $21x10^{-6}$ M) of the studied inhibitors are shown in Figure (8). Similar results were recorded for the other concentrations of the investigated compounds (not shown). The harmonic and intermodulation peaks are clearly visible and are much larger than the background noise. The two large peaks, with amplitude of about 200 µA, are the response to the 40 and 100 mHz (2 and 5 Hz) excitation frequencies. It is important to note that between the peaks there is nearly no current response (<100 nA). The experimental EFM–data were treated using two different models: complete diffusion control of the cathodic reaction and the "activation" model. For the latter, a set of three non-linear equations had been solved, assuming that the corrosion potential does not change due to the polarization of the working electrode [38]. The larger peaks were used to calculate the corrosion current density (j_{corr}), the Tafel slopes (bc and ba) and the causality factors (CF-2 and CF-3).These electrochemical parameters were simultaneously determined by Gamry EFM140 software, and listed in Table 3. The data presented in Table (6) obviously show that, the addition of any one of tested compounds at a given concentration to the acidic solution decreases the corrosion current density, indicating that these compounds inhibit the corrosion of carbon steel in 1 M HCl through adsorption. The causality factors obtained under different experimental conditions are approximately equal to the theoretical values (2 and 3) indicating that the measured data are verified and of good quality [39]. The inhibition efficiencies IE_{EFM} % increase by increasing the studied inhibitor concentrations and was calculated as follows:

$$IE_{EFM}\% = [(1- i_{corr}/ i^{o}_{corr})] \times 100 \quad (5)$$

where i^{o}_{corr} and i_{corr} are corrosion current densities in the absence and presence of inhibitor, respectively. The inhibition sufficiency obtained from this method is in the order: 1 < 2 < 3

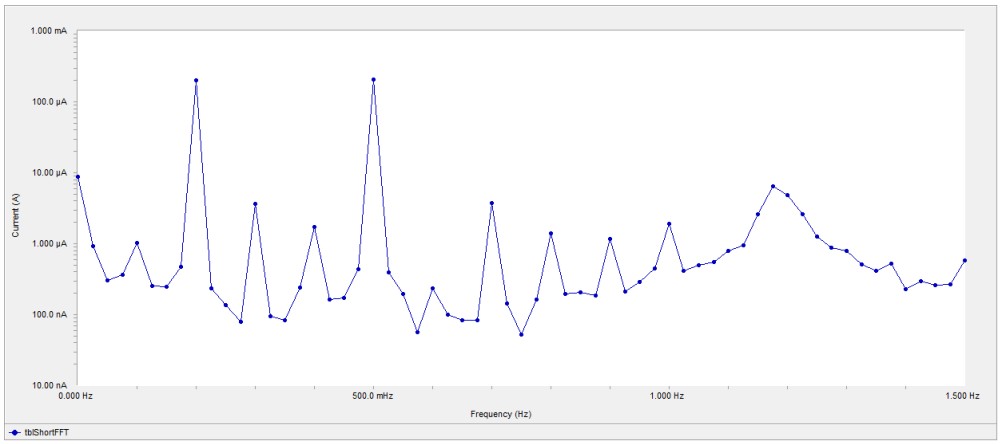

EFM spectra for C-steel in 1 M HCl (blank) at 30˚ C

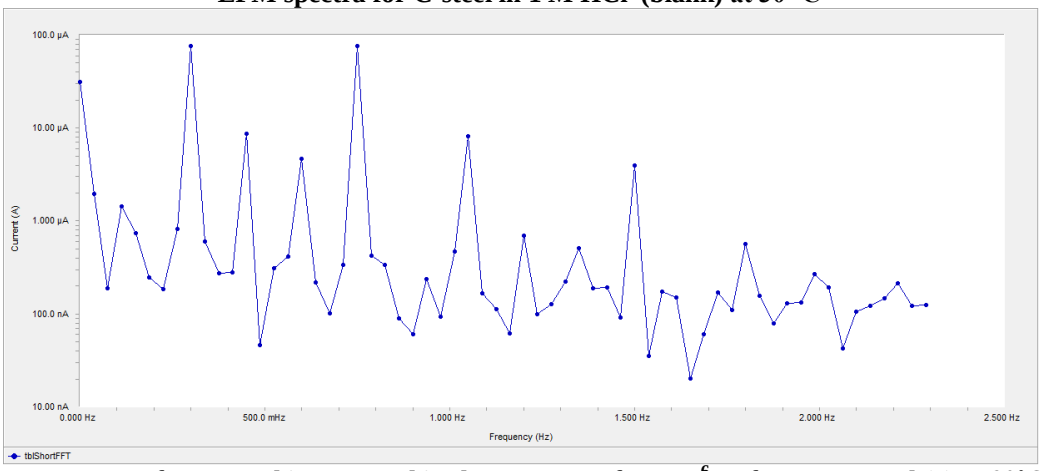

EFM spectra for C- steel in 1 M HCl in the presence of $11x10^{-6}$ M from compond (1) at 30˚C

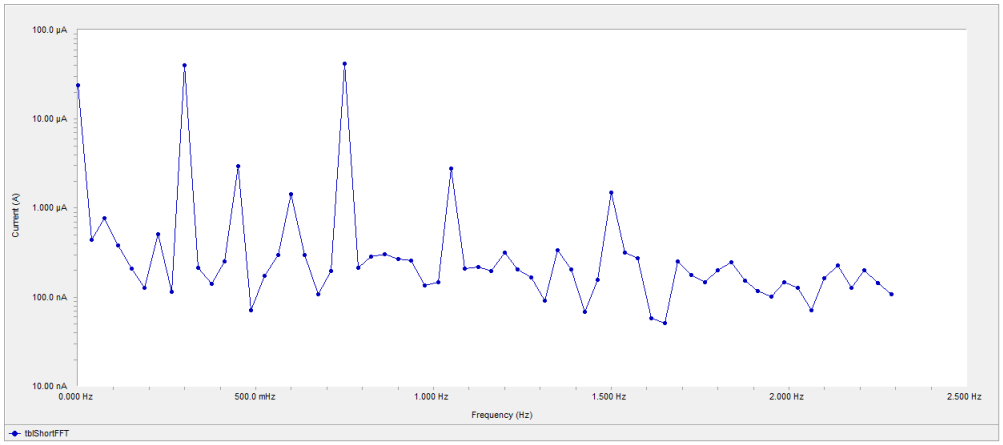

EFM spectra for C- steel in 1 M HCl in the presence of $13x10^{-6}$ M from compond (1) at 30˚ C

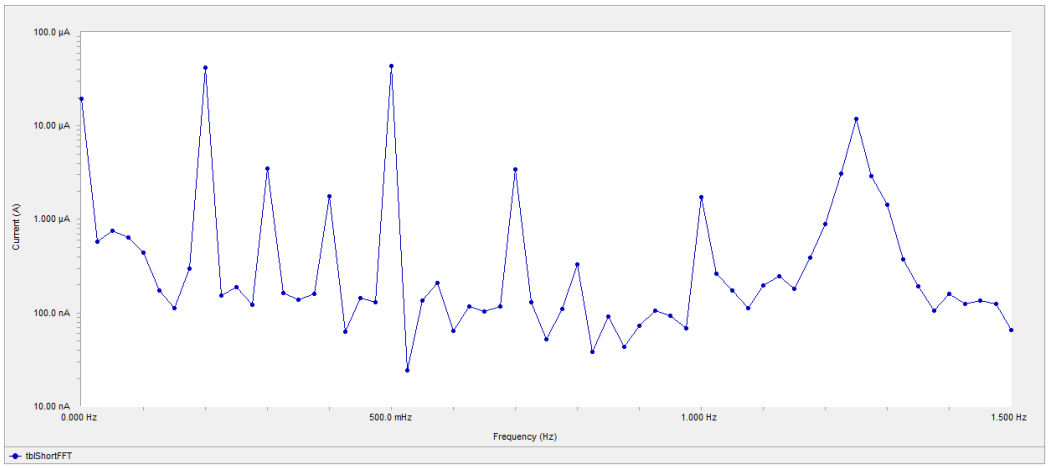

EFM spectra for C- steel in 1 M HCl in the presence of $15x10^{-6}$ M from compond (1) at 30˚ C

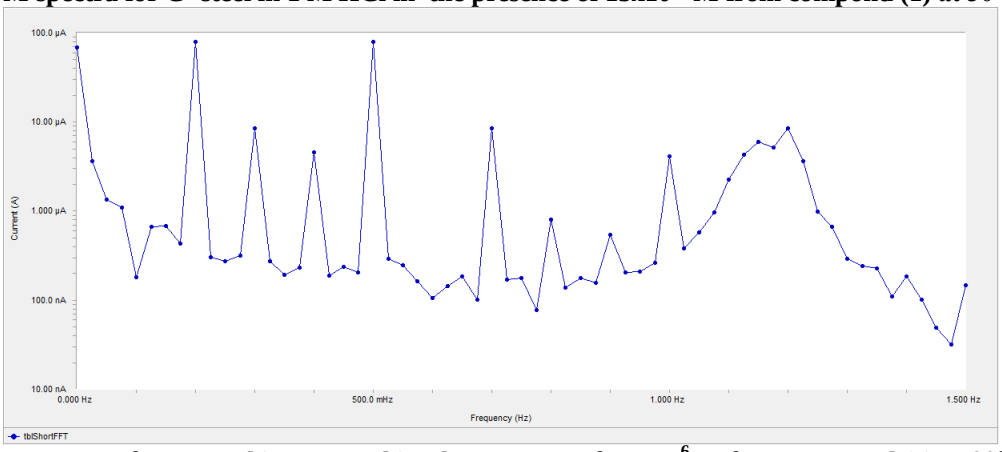

EFM spectra for C- steel in 1 M HCl in the presence of $17x10^{-6}$ M from compond (1) at 30˚ C

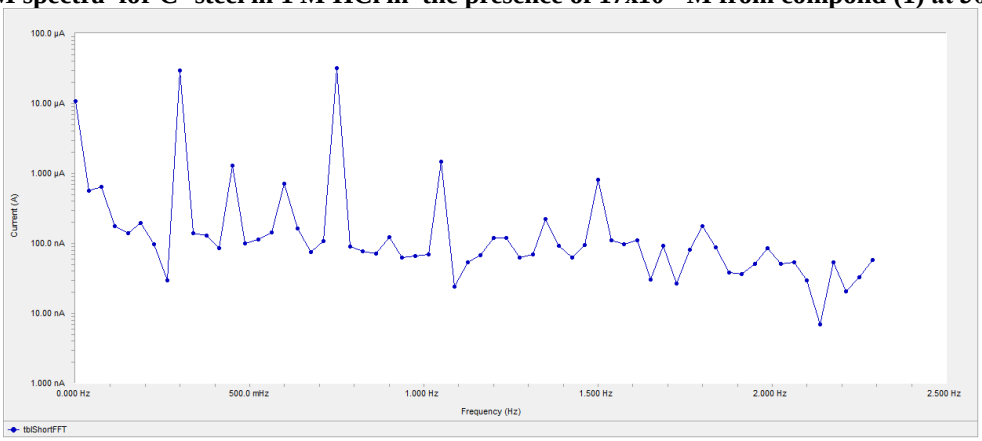

EFM spectra for C- steel in 1 M HCl in the presence of 19 x 10^{-6} M from compond (1) at 30˚ C

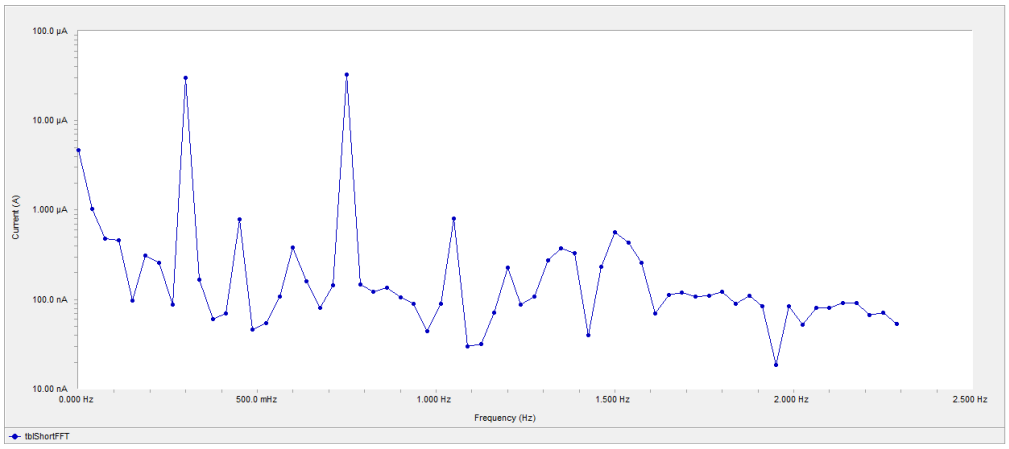

EFM spectra for C-steel in 1 M HCl in the presence of 21 x 10^{-6} M from compond (1) at 30° C

Table (6): Electrochemical kinetic parameters obtained by EFM technique for carbon steel in the absence and presence of various concentrations of inhibitors (1-3) in 1 HCl at 30°C

Comp.	Conc., M	i_{corr} µA cm^{-2}	β_c mV dec^{-1}	β_a mVdec^{-1}	CF-2	CF-3	CR	θ	% IE
1	Blank	355.4	121	107	2.03	3.01	162.4	---	---
	11×10^{-6}	222.9	529	115	1.94	3.91	110	0.373	37.3
	13×10^{-6}	105.5	264	123	1.97	2.29	52.05	0.703	70.3
	15×10^{-6}	85.83	193	98	1.96	2.65	39.54	0.758	75.9
	17×10^{-6}	84.77	90	56	1.95	2.86	39.05	0.761	76.1
	19×10^{-6}	80.57	221	137	1.80	3.01	39.76	0.773	77.3
	21×10^{-6}	69.98	163	130	1.65	3.31	34.53	0.803	80.3
2	11×10^{-6}	69.06	155	128	2.04	3.24	34.08	0.806	80.6
	13×10^{-6}	68.27	152	133	1.74	3.05	33.69	0.808	80.8
	15×10^{-6}	66.07	123	73	1.87	3.17	29.47	0.814	81.4
	17×10^{-6}	56.8	74	70	1.05	3.02	25.95	0.840	84.0
	19×10^{-6}	56.38	133	87	1.85	3.07	27.82	0.841	84.1
	21×10^{-6}	53.12	94	60	1.83	3.18	24.47	0.851	85.1
3	11×10^{-6}	50.92	105	69	1.86	2.93	34.46	0.857	85.7
	13×10^{-6}	46.98	96	65	2.29	2.43	21.65	0.868	86.8
	15×10^{-6}	44.18	55	53	2.66	3.16	20.19	0.876	87.6
	17×10^{-6}	42.85	126	96	1.65	3.41	19.58	0.879	87.9
	19×10^{-6}	39.21	42	37	2.23	2.62	17.92	0.890	89.0
	21×10^{-6}	34.28	42	42	2.08	2.08	15.66	0.904	90.4

3.5. Scanning Electron Microscopy (SEM) Studies

Figure (9) represents the micrography obtained for carbon steel samples in presence and in absence of 21 x 10^{-6} M organic derivatives after exposure for 3 days immersion. It is clear that carbon steel surfaces suffer from severe corrosion attack in the blank sample. It is important to stress out that when the compound is present in the solution, the morphology of carbon steel surfaces is quite different from the previous one, and the specimen surfaces were smoother. We noted the formation of a film which is distributed in a random way on the whole surface of the carbon

steel. This may be interpreted as due to the adsorption of the organic derivatives on the carbon steel surface incorporating into the passive film in order to block the active site present on the carbon steel surface. Or due to the involvement of inhibitor molecules in the interaction with the reaction sites of carbon steel surface, resulting in a decrease in the contact between carbon steel and the aggressive medium and sequentially exhibited excellent inhibition effect [40, 41].

Pure Sample

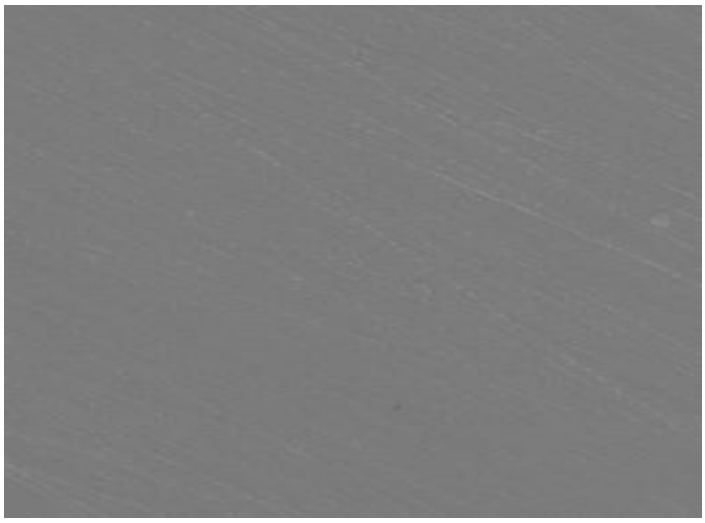

Fig.(3.85):SEM image of C-steel before immersion in 1 M HCl solution

Blank

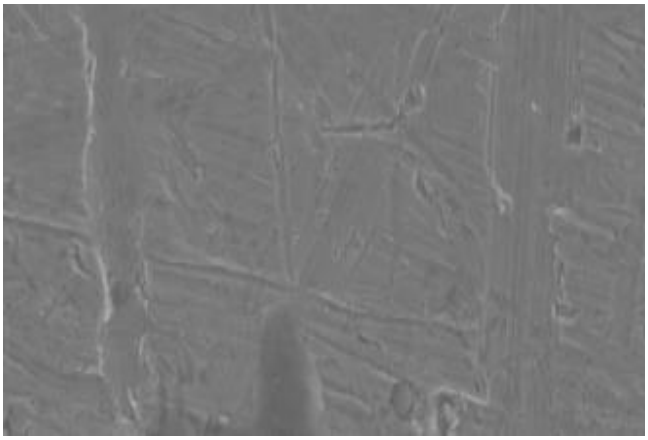

Compound (1)

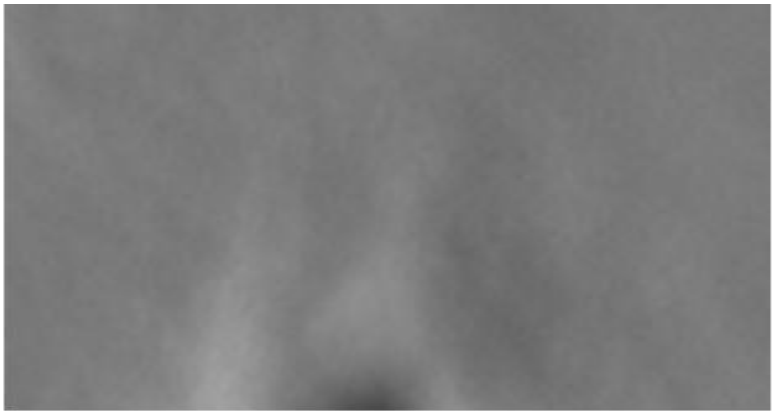

Compound (2)

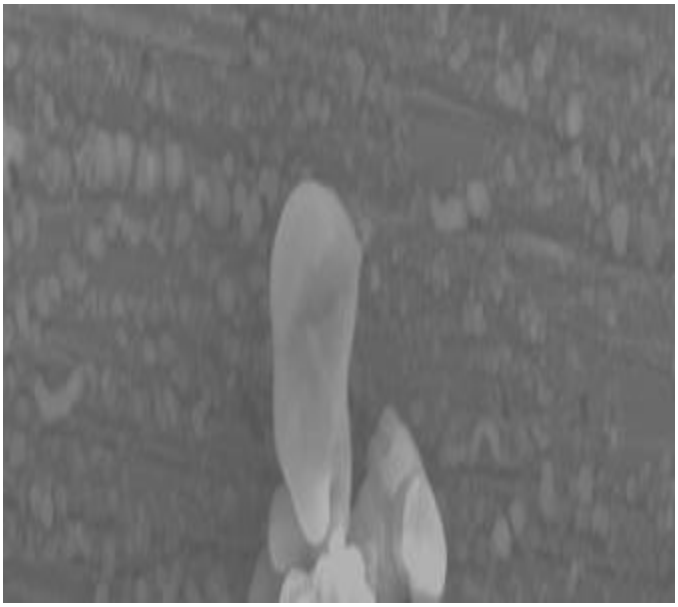

Compound (3)

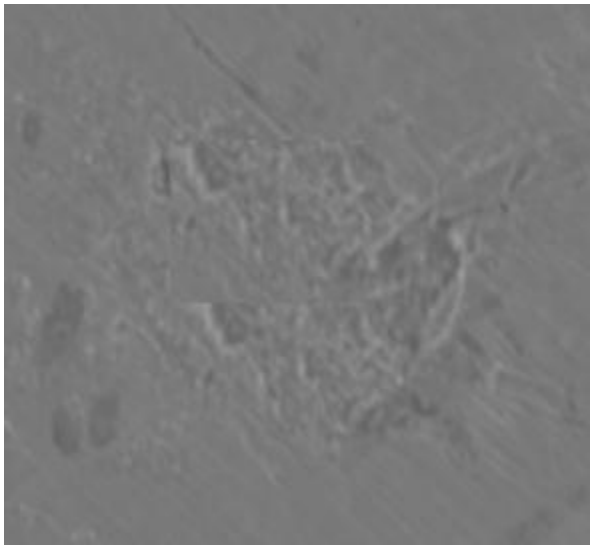

Figure (9): SEM micrographs for C-steel in absence and presence of $21x10^{-6}$ M of investigated compounds

3.6. Energy Dispersion Spectroscopy (EDS) Studies

The EDS spectra were used to determine the elements present on the surface of carbon steel and after 3 days of exposure in the uninhibited and inhibited 1 M HCl. Figure 10 shows the EDS analysis result on the composition of carbon steel only without the acid and inhibitor treatment. The EDS analysis indicates that only Fe and oxygen were detected, which shows that the passive film contained only Fe_2O_3

Pure Sample

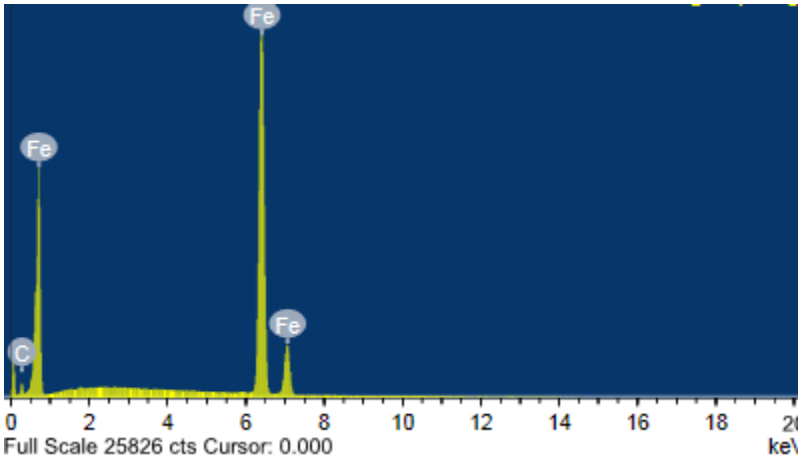

Figure (3.87): EDS analysis of composition of C-steel only without the acid and inhibitor treatment

Blank

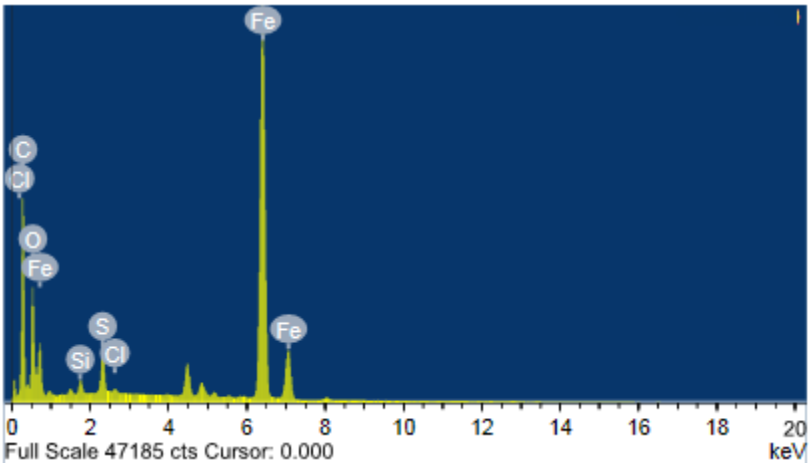

Compound (1)

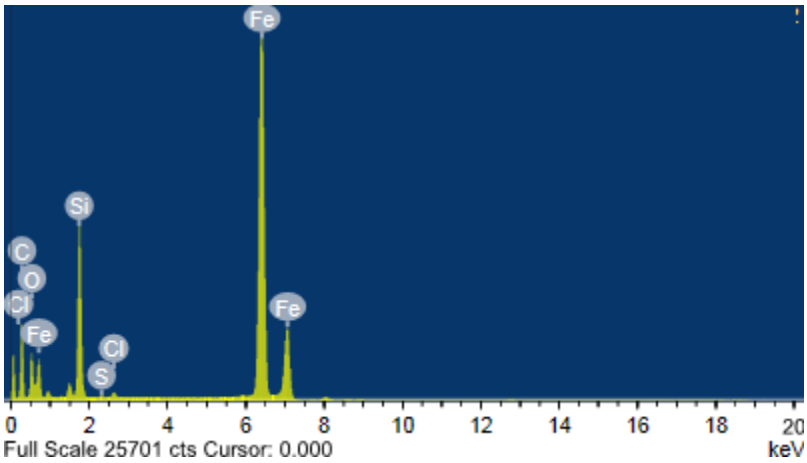

Compound (2)

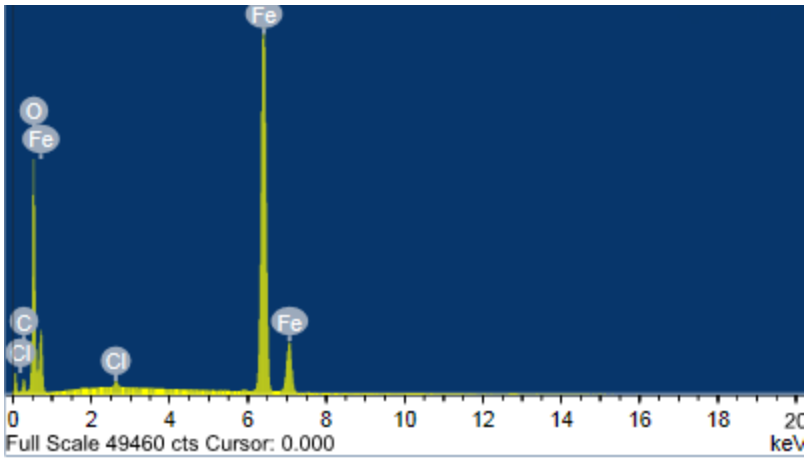

Compound (3)

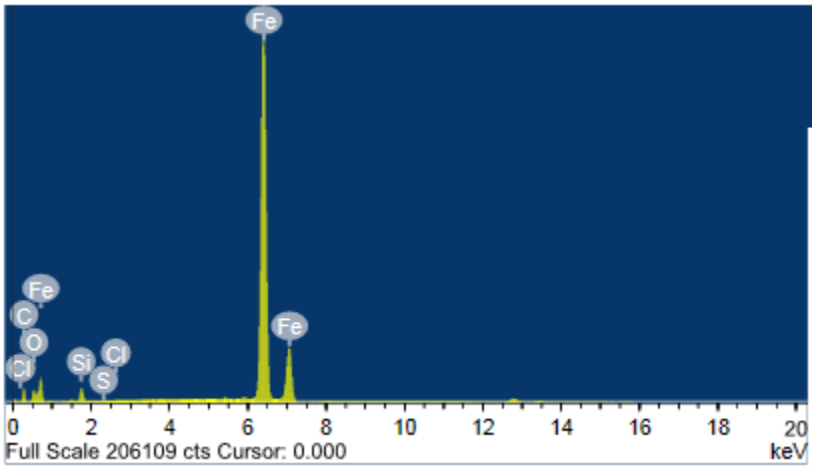

Figure (10): EDX analysis on C-steel in presence and absence of organic compounds for 3 days immersion

Figure (10) portrays the EDX analysis of carbon steel in 1 M HCl only and in the presence of $21x10^{-6}$ M of organic derivatives. The spectra show additional lines, demonstrating the existence of C (owing to the carbon atoms of anhydride derivatives). These data shows that the carbon and O atoms covered the specimen surface. This layer is entirely owing to the inhibitor, because the carbon and O signals are absent on the specimen surface exposed to uninhibited HCl. It is seen that, in addition to Mn, C. and O were present in the spectra. A comparable elemental distribution is shown in Table (7).

Table (7): Surface composition (weight %) of C-steel alloy after 3hrs of immersion in HCl without and with the optimum concentrations of the studied inhibitors

(Mass %)	Fe	C	O	Cl	S	Si
Pure	92.16	7.84	--	--	--	--
blank	21.38	9.23	17	0.35	0.08	0.39
Compound (1)	33.19	9.69	15.29	0.19	0.01	7.62
Compound (2)	43.04	15.29	6.91	0.09	--	--
Compound (3)	70.44	20.82	6.63	0.06	0.09	1.95

3.7. Quantum chemical calculations

Theoretical calculations were performed for only the neutral forms, in order to give further insight into the experimental results. Values of quantum chemical indices such as energies of LUMO and HOMO (E_{HOMO} and E_{LUMO}), the formation heat ΔH_f and energy gap ΔE, are calculated by semi-empirical AM1, MNDO and PM3 methods has been given in Table (8).

The reactive ability of the inhibitor is related to E_{HOMO}, E_{LUMO} [42]. Higher E_{HOMO} of the adsorbent leads to higher electron donating ability [43]. Low E_{LUMO} indicates that the acceptor accepts electrons easily. The calculated quantum chemical indices (EHOMO, ELUMO, μ) of investigated compounds are shown in Table (8). The difference ΔE= ELUMO-EHOMO is the energy required to move an electron from HOMO to LUMO. Low ΔE facilities adsorption of the molecule and thus will cause higher inhibition efficiency.

The bond gap energy ΔE increases from (1 to 3). This fact explains the decreasing inhibition efficiency in this order (1< 2 < 3), as shown in Table (8) and Fig (11) show the optimized structures of the three investigated compounds. So, the calculated energy gaps show reasonably good correlation with the efficiency of corrosion inhibition. Table (8) also indicates that compound (3) possesses the lowest total energy that means that compound

(3) adsorption occurs easily and is favored by the highest softness. The HOMO and LUMO electronic density distributions of these molecules were plotted in Fig (11). For the HOMO of the studied compounds that the benzene ring, N-atoms and O-atom have a large electron density. The data presented in Table (8) show that the calculated dipole moment decrease from (1< 2 < 3).

Structure	HOMO	LUMO
1	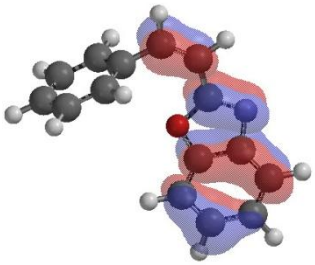	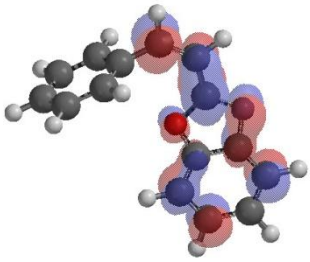
2	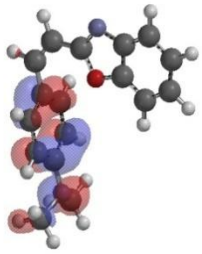	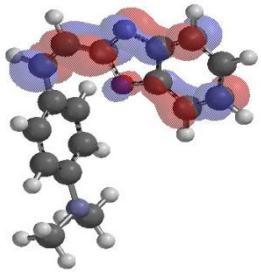
3	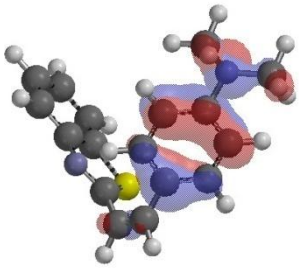	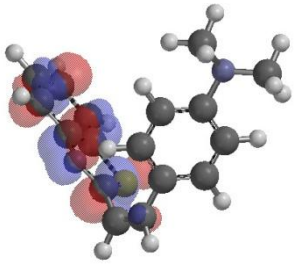

Figure (11): Molecular orbital plots and Mulliken charges of investigated compounds

Table (8): The calculated quantum chemical properties for investigated compounds.

	Compound (1)	Compound (2)	Compound (3)
$-E_{HOMO}$ (eV)	-9.14	-8.50	-8.39
$-E_{LUMO}$ (eV)	-0.72	-0.64	-0.62
ΔE (eV)	8.42	7.86	7.77
Ƞ (eV)	4.21	3.93	3.885
σ (eV^{-1})	0.238	0.254	0.257
-Pi (eV)	-4.93	-4.57	-4.505
χ (eV)	4.93	4.57	4.505
Dipole moment (Debye)	1.68	2.89	1.22
Area ($Å^2$)	254.53	304.58	313.35

3.8- Chemical Structure of the Inhibitors and Corrosion Inhibition

Inhibition of the corrosion of C-steel in 1 M HCl solution by some organic compounds is determined by weight loss, potentiodynamic anodic polarization measurements, Electrochemical Impedance Spectroscopy (EIS), electrochemical frequency modulation method (EFM) and Scanning Electron Microscopy (SEM) Studies, it was found that the inhibition efficiency depends on concentration, nature of metal, the mode of adsorption of the inhibitors and surface conditions. The observed corrosion data in presence of these inhibitors, namely: i) The decrease of corrosion rate and corrosion current with increase in concentration of the inhibitor, ii) The linear variation of weight loss with time, iii) The shift in Tafel lines to higher potential regions, vi) The decrease in corrosion inhibition with increasing temperature indicates that desorption of the adsorbed inhibitor molecules takes place and v) The inhibition efficiency was shown to depend on the number of adsorption active centers in the molecule and their charge density. It was concluded that the mode of adsorption depends on the affinity of the metal towards the π-electron clouds of the ring system. Metals such as Cu and Fe, which have a greater affinity towards aromatic moieties, were found to adsorb benzene rings in a flat orientation. The order of decreasing the percentage inhibition efficiency of the investigated inhibitors in the corrosive solution was as follow: 1 < 2 < 3

Compound (3) exhibits excellent inhibition power due to: (i) its larger molecular size that may facilitate better surface coverage, and (ii) its adsorption through four active centers. Compound (2) comes after compound (3) in inhibition efficiency due to its lower molecular size than compound (3). Compound (1) comes after compound (2) in inhibition efficiency inspite of it has two active centers, because it has lower molecular size than compound (2).

REFERENCES

(1) Thmas, J.G.N. 5th European Symposium on Corrosion Inhibitors, A new triazole derivative as inhibitor of the acid corrosion of mild steel, *Ferrara*, Italy, **1980.**
(2) Donnelly, B.D.C.; Downie T.C.; Grezeskowiak R.,.Hamburg H.R ; Short, D.; The inhibition of mild steel corrosion in acidic medium by 2,2′-bis(benzimidazole), *Corros.Sci.***1977**,18,109
(3) A.B.Tadros and Y.Abdel-Naby, The inhibition effect of the new Schiff base, namely 2, 2′-[bis-N (4-choloro benzaldimin)]-1, 1′-dithio against mild steel corrosion,*J.Electroanal.Chem.*,,**1988**,224,433.
(4) N.C.Subramanyam, B.S.Sheshardi and S.A.Mayanna, Experimental and theoretical investigation of the adsorption behaviour of new triazole derivatives as inhibitors for mild steel corrosion in acid media,*Corros.Sci.***1993**,34,563.
(5) B. Babu, Ramesh, K. Thangavel, dihydropyrimido [2, 1-b][1, 3] thiazine-7-carbonitrile as corrosion inhibitor for carbon steel in acidic media,*Anti-Corros. Meth. Mater.***2005**,52,219.
(6) A.S. Fouda, H.A. Mostafa, F. El-Taib Haekel, G.Y. Elewady, Inhibitive effect of some thiadiazole derivatives on C-steel corrosion in neutral sodium chloride solution, Adsorption and inhibitive properties for corrosion of carbon steel in hydrochloric acid solution by some nicotinonitrile derivatives, *Corros. Sci.* **2005**, 47.
(7) R. Yurchenko, L. Pogrebova, T. Pilipenko, T. Shubina, dihydropyrimido [2, 1-b][1, 3] thiazine-7-carbonitrile as corrosion inhibitor for carbon steel in acidic media, *Russian J. Appl. Chem.***2006,**79, 1100.
(8) S.A. Hossain, A.L. Almarshad, Inhibiting effects of butyl triphenyl phosphonium bromide on corrosion of mild steel in 0.5 M sulphuric acid solution and its adsorption characteristics,Corros. Eng. Sci. Technol.2006, 41, 77.
(9) S.M. Abd El-Wahaab, G.K. Gomma, H.Y. El-Barradie, Anhydride Derivatives as Corrosion Inhibitors for Carbon Steel in Hydrochloric Acid Solutions,*J. Chemical Technol. Biotechnol. 2007,36 ,435.*
(10) S. Muralidharan, S.V.K. Iyer, Corrosion inhibition of mild steel in hydrochloric acid by some aromatic hydrazides, *Anti-Corros. Meth. Mater.1997,44,100.*
(11) M.A. Quraishi, M.A.W. Khan, M. Ajmal, 4-Amino-3-butyl-5-mercapto-1, 2, 4-triazole: a new corrosion inhibitor for mild steel in sulphuric acid,*Anti-Corros. Meth. Mater. 1996,43,5.*
(12) Bentiss, M. Traisnel, M. Lagrenee, Theoretical investigation of the inhibition of corrosion by some triazole Schiff bases,*J. Appl. Electrochem.2001, 31 ,41.*
(13) M. Sahin, S. Bilgic, Pyrazolone derivatives as corrosion inhibitors for C-steel in hydrochloric acid solution,*Anti-Corros. Meth. Mater. 2003, 50 , 34.*
(14) L. Larabi, Y. Harek, M. Traisnel, A. Mansri, Synergistic inhibition between dodecylamine and potassium iodide on the corrosion of cold rolled steel in 0.1 M phosphoric acid, *J. Appl. Electrochem.2004,34 , 833.*
(15) K. Aramaki, M. Hagiwara, H. Nishihara, The synergistic effect of anions and the ammonium cation on the inhibition of iron corrosion in acid solution,*Corros. Sci. 1987,27, 487.*

(16) G. Moretti, G. Quartarone, A. Tassan, A. Zingales, 5-Amino- and 5-chloro-indole as mild steel corrosion inhibitors in 1 N sulphuric acid, Electrochim. Acta, 41, 1971–1980,1996. *International Journal of Advanced Research 2013, 1(10) 568-588*
(17) M. Dudukcu, B. Yazici, M. Erbil, The effect of indole on the corrosion behaviour of stainless steel,*Mater. Chem. Phys. 2004, 87, 138–141*.
(18) A. A. Ismail, S. H. Sanad, A. A. El-Meligi, inhibiting effect of indole and some of its derivatives on corrosion of C-steel in HCl, *J. Mater. Sci. Technol. 2000,16 397-400.*
(19) L. Wang, Evaluation of 2-mercaptobenzimidazole as corrosion inhibitor for mild steel in phosphoric acid, *Corros. Sci. 2001 ,43, 2281–2289,*
(20) A. Popova, M. Christov, T. Deligeorigiev, Influence of the Molecular Structure on the Inhibitor Properties of Benzimidazole Derivatives on Mild Steel Corrosion in 1 M Hydrochloric Acid. *Corrosion 2003 ,59, 756–764.*
(21) A. Popova, M. Christov, S. Raicheva, E. Sokolova, Adsorption and inhibitive properties of benzimidazole derivatives in acid mild steel corrosion, *Corros. Sci.2004,46,1333–1350.*
(22) R. W. Bosch, J. Hubrecht, W. F. Bogaerts, B. C. Syrett, Electrochemical frequency modulation as a new technique for monitoring corrosion inhibition of iron in acid media by new thiourea derivative, *Corrosion 2001,57, 60.*

(23) S. S. Abdel–Rehim, K. F. Khaled, N. S. Abd–Elshafi, Electrochemical frequency modulation and inductively coupled plasma atomic emission spectroscopy methods for monitoring corrosion rates and inhibition of low alloy steel corrosion in HCl solutions and a test for validity of the Tafel extrapolation method,*Electrochim. Acta 2006,51,3269.*

(24) E.Khamis, Temperature effects on the corrosion inhibition of mild steel in acidic solutions by aqueous extract of fenugreek leaves,*Corrosion, 1990,46 ,476.*
(25) F. Bensajjay, S. Alehyen, M. El Achouri,S. Kertit, Ziziphus mauritiana leaves extracts as corrosion inhibitor for mild steel in H2SO4 and HCl solutions,*Anti-Corros. Meth. Mater.2003,50 ,402.*

(26) S.Z. Duan, Y.L Tao, Inhibition of C38 steel corrosion in hydrochloric acid solution by 4, 5-Diphenyl-1H-Imidazole-2-Thiol: Gravimetric and temperature effects treatments,*Interface Chem. Higher Education Press, Beijing,1990,124.*
(27) S.S. Abd El-Rehim, S.A.M. Refaey, F. Taha, M.B. Saleh, R.A. Ahmed, Corrosion inhibition of mild steel in acidic medium using 2-amino thiophenoland 2-cyanomethyl benzothiazole, *J. Appl. Electrochem. 2001, 31 ,429.*
(28) K.K. Al-Neami, A.K. Mohamed, I.M. Kenawy, A.S. Fouda, Pyrazolone derivatives as corrosion inhibitors for C-steel in hydrochloric acid solution, *Monatsh Chem. 1995, 126 , 369.*
(29) K. Haladky, L. Collow, J. Dawson, Br. Corrosion and Inhibition of 316L stainless steel in neutral medium by 2-Mercaptobenzimidazole,*Corros. J. 1980, 15 ,20.*
(30) S.S. Abd El-Rehim, M.A.M. Ibrahim, K.F. Khaled, 4-Aminoantipyrine as an inhibitor of mild steel corrosion in HCl solution, *J. Appl. Electrochem. 1999, 29, 593.*
(31) A.S. Fouda, A.A. Al-Sarawy, M.S. Radwan, Role of some thiadiazole derivatives as inhibitors for the corrosion of C-steel in 1 M H2SO4,*Ann. Chim. 2006, 96 , 85.*
(32) A.K. Mohamed, H.A. Mostafa, G.Y. El-Awady, A.S. Fouda, Anhydride Derivatives as Corrosion Inhibitors for Carbon Steel in Hydrochloric Acid Solutions,*Port. Electrchim. Acta, 2000, 18 , 99.*
(33) A. El-Ouafi, B. Hammouti, H. Oudda, S. Kerit, R. Touzani, A. Ramdani, Role of some thiadiazole derivatives as inhibitors for the corrosion of C-steel in 1 M H_2SO_4,*Anti-Corros. Meth. Mater. 2002, 49, 199.*
(34) F. Mansfeld, M.W. Kendig, S. Recording and Analysis of AC Impedance Data for Corrosion Studies, *Tsai, Corros. 1982, 38 , 570.*
(35) F. Mansfeld, heterocyclic amines and derivatives as corrosion inhibitors for iron in perchloric acid,*Eletrochim. Acta, 1990,35 , 1533.*
(36) E. McCafferty, N Hackerman, Double layer capacitance of iron and corrosion inhibition with polymethylene diamines,*J. Electrochem. Soc. 1972,119 , 146.*
(37) E. Kus, F. Mansfeld, A study of the inhibition of iron corrosion in HCl solutions by some amino acids, *Corros. Sci. 2006, 48 , 965.*

(38) G. A. Caigman, S. K. Metcalf, E. M. Holt, Anhydride Derivatives as Corrosion Inhibitors for Carbon Steel in Hydrochloric Acid Solutions,*J.Chem. Cryst. 2000,30 , 415.*

(39) D.C. Silverman and J.E. Carrico, Corrosion of reinforcements in artificial sea water and concentrated sulfate solution, *National Association of Corrosion Engineers, 1988,44 , 280.*
(40) R.A., Prabhu, T.V., Venkatesha, A.V., Shanbhag, G.M., Kulkarni, R.G., Kalkhambkar, Inhibition effect of Amoxycillin drug on the corrosion of mild steel in 1 N hydrochloric acid solution,*Corros.Sci.2008, 50, 3356.*

(41) G., Moretti, G., Quartanone, A., Tassan, A., Zingales, , Wekst. Korros. Quinazoline Derivatives as Green Corrosion Inhibitors for Carbon Steel in Hydrochloric Acid Solutions, *1994, 45, 641*
(42) C. Lee, W. Yang and R. G. Parr. Ab initio characterization of phenylnitrenium and phenylcarbene: remarkably different properties for isoelectronic species, Phys. Rev. B *1988 ,37,785.*
(43) R. M. Issa, M. K. Awad and F. M. Atlam, Quantum chemical studies on the inhibition of corrosion of copper surface by substituted uracils,*Appl. Surf. Sci. 2008, 255, 2433.*